bioRxiv preprint doi: https://doi.org/10.1101/038281; this version posted January 30, 2016. The copyright holder for this preprint (which was not certified by peer review) is the author/funder, who has granted bioRxiv a license to display the preprint in perpetuity. It is made available under aCC-BY-NC 4.0 International license.

Compaction and segregation of sister chromatids via active loop extrusion

Anton Goloborodko[1], Maxim V. Imakaev[1], John F. Marko[2], and Leonid Mirny[1,3,*]

Short title: Compaction and segregation of sister chromatids

[1] *Department of Physics, Massachusetts Institute of Technology, Cambridge MA 02139*

[2] *Department of Molecular Biosciences and Department of Physics and Astronomy, Northwestern University, Evanston IL 60208*

[3] *Institute for Medical Engineering & Science, Massachusetts Institute of Technology, Cambridge MA 02139*

[*] *Corresponding author*: Leonid Mirny, Institute for Medical Engineering & Science, Massachusetts Institute of Technology, 77 Mass Ave, Cambridge MA 02139, leonid@mit.edu, +16174524862

Keywords: prophase, polymers, condensin, structural maintenance of chromosomes

bioRxiv preprint doi: https://doi.org/10.1101/038281; this version posted January 30, 2016. The copyright holder for this preprint (which was not certified by peer review) is the author/funder, who has granted bioRxiv a license to display the preprint in perpetuity. It is made available under aCC-BY-NC 4.0 International license.

Abstract

The mechanism by which chromatids and chromosomes are segregated during mitosis and meiosis is a major puzzle of biology and biophysics. Using polymer simulations of chromosome dynamics, we show that a single mechanism of loop extrusion by condensins can robustly compact, segregate and disentangle chromosomes, arriving at individualized chromatids with morphology observed *in vivo*. Our model resolves the paradox of topological simplification concomitant with chromosome "condensation", and explains how enzymes a few nanometers in size are able to control chromosome geometry and topology at micron length scales. We suggest that loop extrusion is a universal mechanism of genome folding that mediates functional interactions during interphase and compacts chromosomes during mitosis.

bioRxiv preprint doi: https://doi.org/10.1101/038281; this version posted January 30, 2016. The copyright holder for this preprint (which was not certified by peer review) is the author/funder, who has granted bioRxiv a license to display the preprint in perpetuity. It is made available under aCC-BY-NC 4.0 International license.

Introduction

The mechanism whereby eukaryote chromosomes are compacted and concomitantly segregated from one another remains poorly understood. A number of aspects of this process are remarkable. First, the chromosomes are condensed into elongated structures that maintain the linear order, i.e. the order of genomic elements in the elongated chromosome resembles their order along the genome (1). Second, the compaction machinery is able to distinguish different chromosomes and chromatids, preferentially forming intra-chromatid cross-links: if this were not the case, segregation would not occur (2). Third, the process of compaction is coincident with segregation of sister chromatids, i.e. formation of two separate chromosomal bodies. Finally, originally intertwined sister chromatids become topologically disentangled, which is surprising, given the general tendency of polymers to become *more* intertwined as they are concentrated (3).

None of these features cannot be produced by indiscriminate cross-linking of chromosomes (4), which suggests that a novel mechanism of polymer compaction must occur, namely “lengthwise compaction” (3, 5, 6), which permits each chromatid to be compacted while avoiding sticking of separate chromatids together. Cell-biological studies suggest that topoisomerase II and condensin are essential for metaphase chromosome compaction (7–10), leading to the hypothesis that mitotic compaction-segregation relies on the interplay between the activities of these two protein complexes. Final structures of mitotic chromosomes were shown to consist arrays of consecutive loops (11–13). Formation of such arrays would naturally results in lengthwise chromosome compaction.

One hypothesis of how condensins can generate compaction without crosslinking of topologically distinct chromosomes is that they bind to two nearby points and then slide to generate a progressively larger loop (2). This type of “loop extrusion” kinetics can generate chromatin loops that are stabilized by multiple “stacked” condensins (14) making them robust against the known dynamic binding-unbinding of individual condensin complexes (15). Simulations of this system at larger scales (16) have established that there are two regimes of steady-state dynamics in this system of exchanging loop-extruding factors: (i) a sparse regime where little compaction is achieved and, (ii) a dense regime where a dense array of stabilized loops is created. However, these two quantitative studies (14, 16) focused on the hierarchy of extruded loops and did not consider the 3D conformation and topology of the chromatin fiber in the formed loop arrays. The question of whether loop-extruding factors can act on a chromatin fiber so as to form an array of loops, driving chromosome compaction and chromatid segregation, as originally hypothesized for condensin in (2), is salient and unanswered. The main objective of this paper is to test this hypothesis and to understand how formation of extruded loop arrays ultimately leads to compaction, segregation and disentanglement (topology simplification) of originally intertwined sister chromatids.

Here we use large-scale polymer simulations to show that active loop extrusion in

bioRxiv preprint doi: https://doi.org/10.1101/038281; this version posted January 30, 2016. The copyright holder for this preprint (which was not certified by peer review) is the author/funder, who has granted bioRxiv a license to display the preprint in perpetuity. It is made available under aCC-BY-NC 4.0 International license.

presence of topo II is sufficient to reproduce robust lengthwise compaction of chromatin into dense, elongated, prophase chromatids with morphology in quantitatively accord with experimental observations. Condensin-driven lengthwise compaction, combined with the strand passing activity of topo II drives disentanglement and segregation of sister chromatids in agreement with theoretical prediction that linearly compacted chromatids must spontaneously disentangle (3).

Model

We consider a chromosome as a flexible polymer, coarse-graining to monomers of 10 nm diameter, each corresponding to three nucleosomes (600bp). As earlier (13, 17), the polymer has a persistence length of ~5 monomers (3Kb), is subject to excluded volume interactions and to the activity of loop-extruding condensin molecules and topo II (see below, and in (17)). We simulate chains of 50000 monomers, which corresponds to 30 Mb, close to the size of the smallest human chromosomal arm.

Each condensin complex is modeled as a dynamic bond between a pair of monomers that is changed as a function of time (**Figure 1, Video 1**). Upon binding, each condensin forms a bond between two adjacent monomers; subsequently both bond ends of a condensin move along the chromosome in opposite directions, progressively bridging more distant sites and effectively extruding a loop. As in prior lattice models of condensins (14, 16), when two condensins collide on the chromatin, their translocation is blocked; equivalently, only one condensin is permitted to bind to each monomer, modeling their steric exclusion. Exchange of condensins between chromatin and solution is modeled by allowing each condensin molecule to stochastically unbind from the polymer. To maintain a constant number of bound condensins, when one condensin molecule dissociates, another molecule associates at a randomly chosen location, including chromatin within loops extruded by other condensins. This can potentially lead to formation of reinforced loops (**Video 2,** see below) (14, 16).

bioRxiv preprint doi: https://doi.org/10.1101/038281; this version posted January 30, 2016. The copyright holder for this preprint (which was not certified by peer review) is the author/funder, who has granted bioRxiv a license to display the preprint in perpetuity. It is made available under aCC-BY-NC 4.0 International license.

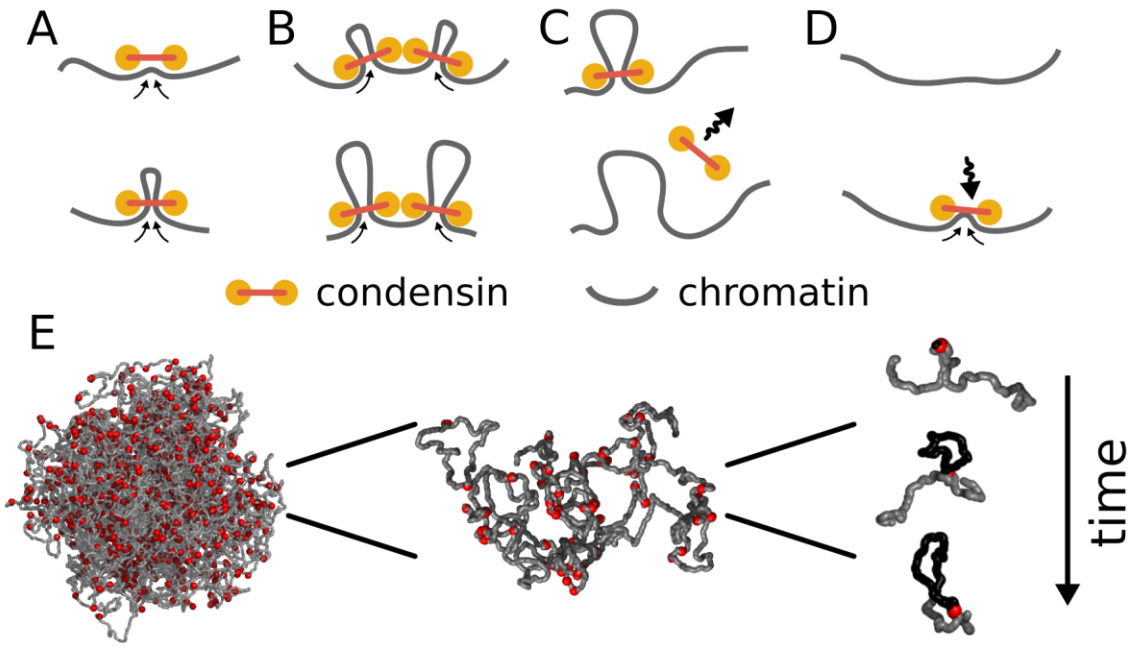

Figure 1. Model of loop extrusion by condensins. Top row, the update rules used in simulations: (**A**) a condensin extrudes a loop by moving the two ends along the chromosome in the opposite directions, (**B**) collision of condensins bound to chromosomes blocks loop extrusion on the collided sides, (**C**) a condensin spontaneously dissociates and the loop disassembles; (**D**) a condensin associates at randomly chosen site and starts extruding a loop. Bottom row, (**E**) we study how combined action of many loop extruding condensins changes the conformation of a long chromosome using polymer simulations.

To simulate the strand-passing activity of topo II enzymes, we permit crossings of chromosomal fiber by setting a finite energy cost of fiber overlaps. By adjusting the overlap energy cost we can control the rate at which topology changes occur.

This model has seven parameters. Three describe the properties of the chromatin fiber (linear density, fiber diameter, and persistence length); two control condensin kinetics (the mean linear separation between condensins, and their processivity, i.e. the average size of a loop formed by an isolated condensin before it dissociates, and defined as two times the velocity of bond translocation times the mean residence time); one parameter controls the length of the monomer-monomer bond mediated by a condensin (effectively the size of a condensin complex), and finally we have the energy barrier to topological change.

The effects of two of these parameters, linear separation of condensins and their processivity, have been considered earlier in the context of a 1D model (16). These parameters control the fraction of a chromosome extruded into loops and the average loop length. In our simulations, we use the separation of 30kb (1000 condensins per 30 Mb chromosome, as measured in (18)) and the processivity of 830 kb such that condensins form a dense array of gapless loops with the average loop length of 100kb, which agrees with available experimental observations (11–13, 19). The effects of the

bioRxiv preprint doi: https://doi.org/10.1101/038281; this version posted January 30, 2016. The copyright holder for this preprint (which was not certified by peer review) is the author/funder, who has granted bioRxiv a license to display the preprint in perpetuity. It is made available under aCC-BY-NC 4.0 International license.

other five parameters are considered below.

Initially, chromosomes are compacted to the density of chromatin inside the human nucleus and topologically equilibrated, thus assuming an equilibrium globular conformation, corresponding to a chromosomal territory. In the simulations of sister chromatid segregation, the initial conformation of one chromatid is generated as above, while the second chromatid traces the same path at a distance of 50nm and winds one full turn per 100 monomers (60 kb). In this state, two chromatids run parallel to each other and are highly entangled, while residing in the same chromosome territory. This represents to the most challenging case for segregation of sister chromatids.

Results

Loop extrusion compacts randomly coiled interphase chromosomes into prophase-like chromosomes

Our main qualitative result is that loop extrusion by condensins and strand passing mediated by topo II convert initially globular interphase chromosomes into elongated, unknotted and relatively stiff structures that closely resemble prophase chromosomes (**Figure 2, Video 2, Supplemental Figure 1**). The compacted chromosomes have the familiar “noodle” morphology (**Figure 2BC**) of prophase chromosomes observed in optical and electron microscopy (20, 21). Consistent with the observed linear organization of prophase chromosomes, our simulated chromosomes preserve the underlying linear order of the genome (**Figure 2C, Supplemental Figure 2**), (20–24). Moreover, the geometric parameters of our simulated chromosomes match the experimentally measured parameters of mid-prophase chromosomes (**Figure 2B**): both simulated and human chromosomes have a linear compaction density ~5 kb/nm (20) and the radius of 300nm (25–27).

bioRxiv preprint doi: https://doi.org/10.1101/038281; this version posted January 30, 2016. The copyright holder for this preprint (which was not certified by peer review) is the author/funder, who has granted bioRxiv a license to display the preprint in perpetuity. It is made available under aCC-BY-NC 4.0 International license.

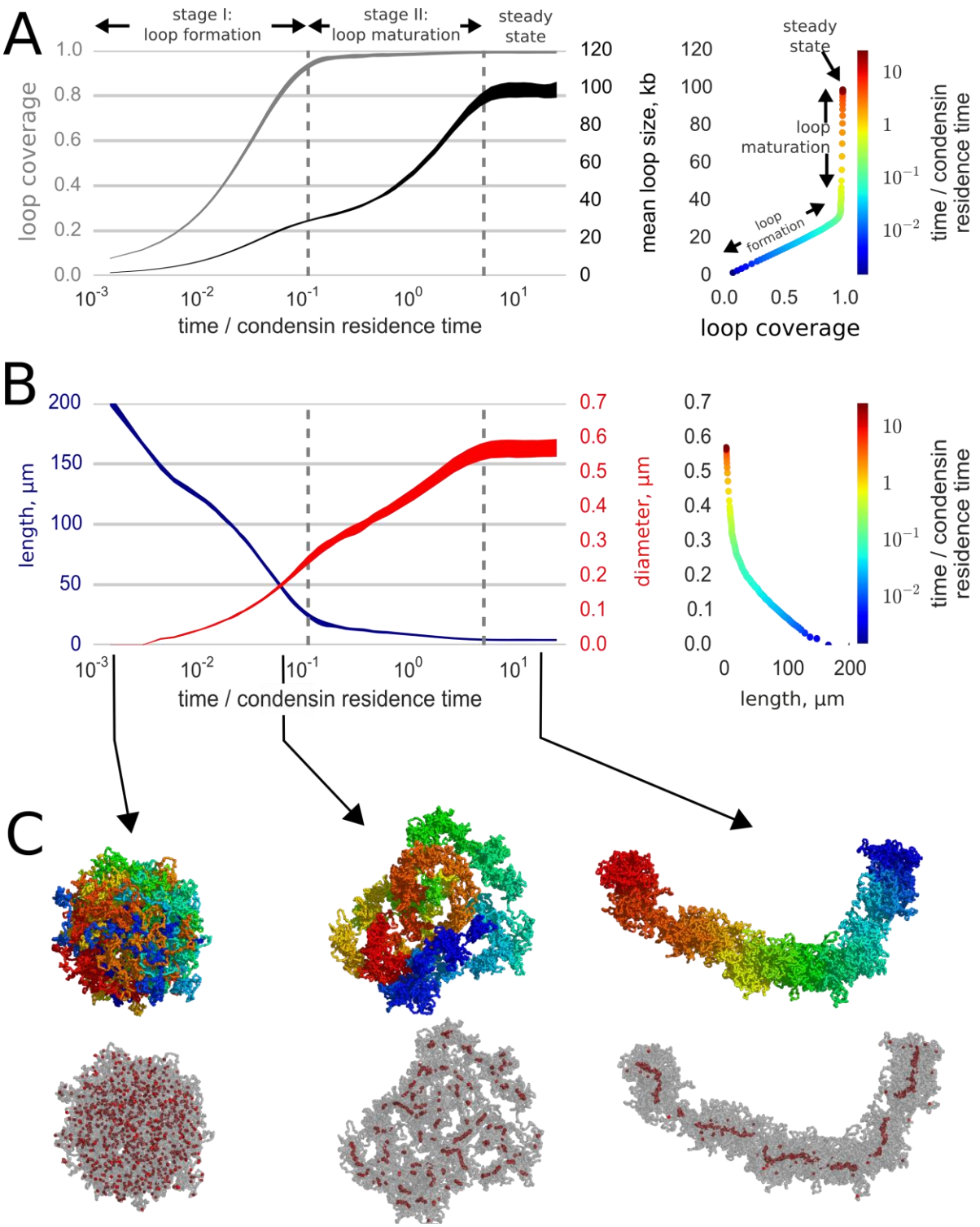

Figure 2. Loop-extruding condensins convert globular interphase chromosomes into elongated structures. (**A**) Dynamics of loop array formation. Left, the fraction of the chromosome extruded into loops (loop coverage, gray) and the mean loop size (black). The time is measured in the units of condensin residence time. Data for each curve was obtained using 10 simulation replicas; the thickness of each line shows the difference between the 10th and 90th percentile at each time point. Right, a phase diagram showing loop coverage vs mean loop length. The curve is averaged over the simulation replicas and colored by log-time. Two stages of dynamics are separated by the two vertical dashed lines corresponding to 95% coverage and 95% of the steady state mean loop length. The distinction between the two stages of compaction is especially easy to see on the phase curve. (**B**) Dynamics of chromosome morphology. Left: chromosome length

bioRxiv preprint doi: https://doi.org/10.1101/038281; this version posted January 30, 2016. The copyright holder for this preprint (which was not certified by peer review) is the author/funder, who has granted bioRxiv a license to display the preprint in perpetuity. It is made available under aCC-BY-NC 4.0 International license.

(blue) and the mean chromosome diameter (red) shown as a function of time; the thickness of each line shows the difference between the 10th and 90th percentile at each time point. Right, a phase diagram showing chromosome length vs diameter; the curve is averaged over the simulation replicas and colored by log-time. Note that most of chromosome linear compaction is achieved during the first phase, while the second is characterized by widening of the chromosome and further three-fold shortening. (**C**) Snapshots of polymer simulations. Top row: the conformations of chromosomes at the beginning of simulations (left), slightly before the transition between the loop formation and maturation stages (middle), and in the steady state (right). Color (rainbow: from red to blue) shows positions of individual monomers along the chain and demonstrates that loci in compacted chromosomes are arranged linearly according to their genomic location. Bottom row: same as above, with chromosomes shown in semitransparent gray and condensins as red spheres.

The internal structure of compacted chromosomes also agrees with structural data for mitotic chromosomes. First, loop extrusion compacts a chromosome into a chain of consecutive loops (16), which agrees with a wealth of microscopy observations (11, 12, 28) and the recent Hi-C study (13). Second, our polymer simulations show that a chain of loops naturally assumes a cylindrical shape, with loops forming the periphery of the cylinder and loop-extruding condensins at loop bases forming the core (**Figure 2c**, **Video 2**), as was predicted in (2). Condensin-staining experiments reveal similar cores in the middle of in vivo and reconstituted mitotic chromosomes (28, 29). In agreement with experiments where condensin cores appear as early as late prophase (27), we observe rapid formation of condensin core in simulations (**Figure 2, Video 2**). Thus, the structure of chromosomes compacted by loop extrusion is consistent with the loop-compaction picture of mitotic (11, 29, 30) and meiotic chromosomes (31, 32). However, it should be noted that our model does not rely on a connected “scaffold”, and that cleavage of the DNA will result in disintegration of the entire structure, as is observed experimentally (33).

Loop-extrusion generates chromosome morphology kinetics similar to those observed experimentally

Simulations also reproduce several aspects of compaction kinetics observed experimentally. First, the model shows that formed loops are stably maintained by condensins despite their constant exchange with the nucleoplasm (8, 15, 34). This stability is achieved by accumulation of several condensins at a loop base (14, 16). Supported by multiple condensins, each loop persists for times much longer than the residency time for individual condensins (16).

Second, simulations show that chromosome compaction proceeds by two stages (**Figure 2AB**): fast formation of a loose, elongated morphology, followed by a slow maturation stage. During the initial “loop formation stage”, condensins associate with the chromosome and extrude loops until colliding with each other, rapidly compacting the chromosome (**Figure 2, Video 2**). At the end of this stage, that takes a fraction of the condensin exchange time, a gapless array of loops is formed, the loops are relative small, supported by single condensins, and the chromosome is long and thin (**Figure 2B**).

bioRxiv preprint doi: https://doi.org/10.1101/038281; this version posted January 30, 2016. The copyright holder for this preprint (which was not certified by peer review) is the author/funder, who has granted bioRxiv a license to display the preprint in perpetuity. It is made available under aCC-BY-NC 4.0 International license.

During the following "maturation stage", due to condensin exchange some loops dissolve while others grow and get reinforced by multiple condensins. As the mean loop size grows (**Figure 2A**), the chromosome becomes thicker and shorter. By the end this stage, which takes several rounds of condensin exchange, the chromosome achieves a steady state where loops get reinforced by multiple condensins and the average loop size and the lengthwise compaction reach their maximal values (**Figure 2**).

These dynamics are in accord with the observation that chromosomes rapidly attain a condensed "noodle"-like shape in early prophase, then spend the rest of prophase growing thicker and shorter (20, 21, 27, 35) (see Discussion).

Loop extrusion separates and disentangles sister chromatids

In a second set of simulations, we studied whether loop extrusion and strand passing simultaneously lead to spatial segregation (2) and disentanglement of sister chromatids (5). We simulated two long polymers connected at their midpoints that represented sister chromatids with stable centromeric cohesion. To model cohesion of sister chromatids in late G2 phase we further twisted them around each other (see Methods) while maintaining them with a chromosomal territory.

We find that the activity of loop-extruding condensins in the presence of topo II leads to compactions of each of the sister chromatids into prophase-like "noodle" structures (**Video 3**). Moreover, we observe that formed compact chromosomes (a) become segregated from each other, as evident by the drastic growth of the mean distance between their backbones (**Figure 3A**), and (b) become disentangled, as shown by the reduction of the winding number of their backbones (**Figure 3B**). Thus, loop extrusion and strand passing folds highly catenated sister chromatids into separate disentangled structures. (**Figure 3C, Video 3**).

bioRxiv preprint doi: https://doi.org/10.1101/038281; this version posted January 30, 2016. The copyright holder for this preprint (which was not certified by peer review) is the author/funder, who has granted bioRxiv a license to display the preprint in perpetuity. It is made available under aCC-BY-NC 4.0 International license.

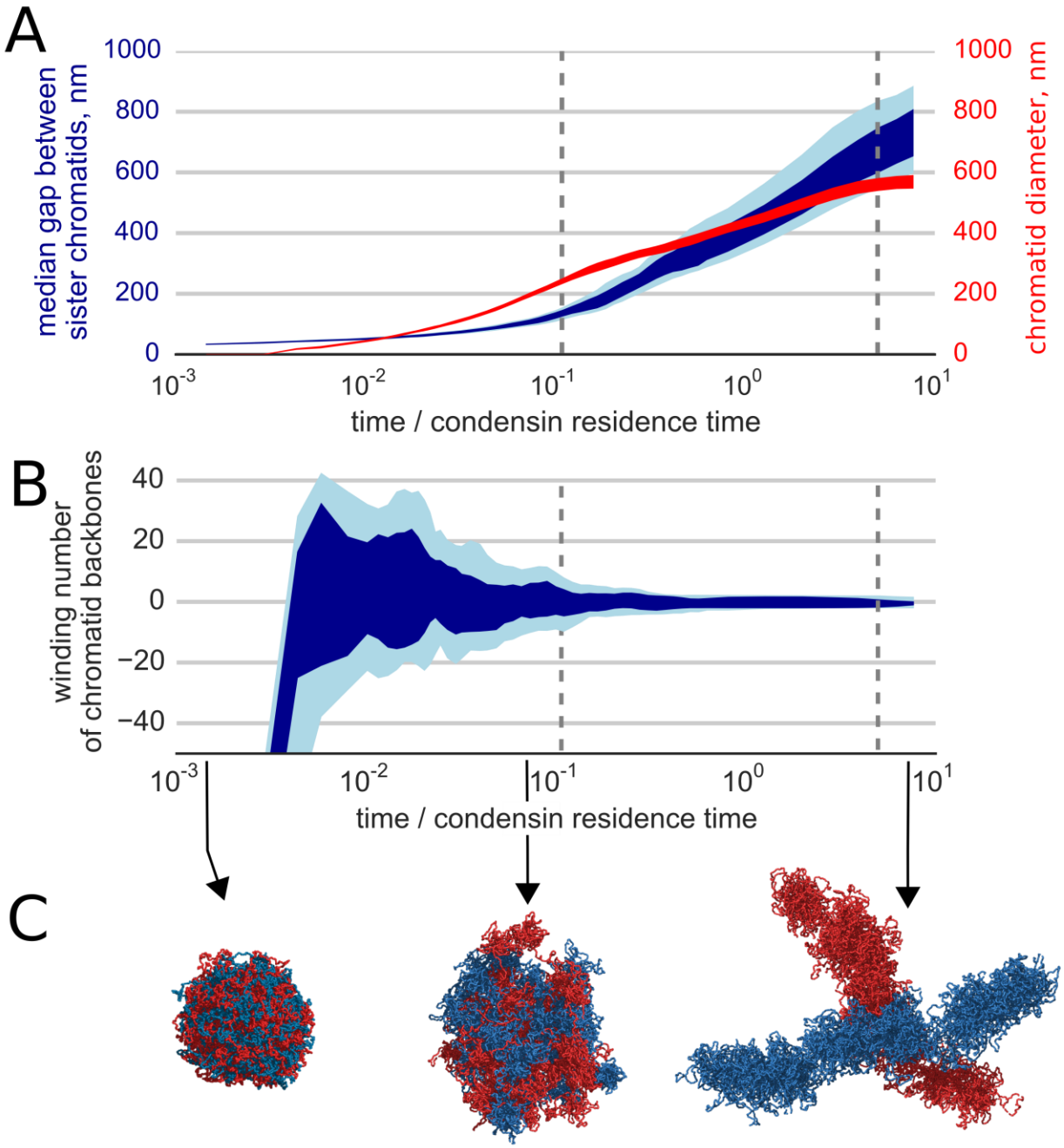

Figure 3. Segregation and disentanglement of sister chromatids. (**A**) The mean separation between sister chromosomes (blue) and the mean chromosome diameter (red) as a function of time, measured in condensin residence times, as above. The blue band shows the range between 25th and 75th percentile at each time point; the light blue shows 10%--90% range. (**B**) Entanglement of sister chromatids measured by the linking number of the condensin cores of sister chromatids. (**C**) Conformations of two sister chromatids in the polymer simulations (shown in red and blue) illustrate the observed segregation and disentanglement.

Despite stochastic dynamics of condensins, compaction, segregation and disentanglement of sister chromatids are highly reproducible and robust to changes in simulation parameters. Disentanglement and segregation were observed in each of 16 simulation replicas (**Video 4**). We also performed simulations with altered chromatin

bioRxiv preprint doi: https://doi.org/10.1101/038281; this version posted January 30, 2016. The copyright holder for this preprint (which was not certified by peer review) is the author/funder, who has granted bioRxiv a license to display the preprint in perpetuity. It is made available under aCC-BY-NC 4.0 International license.

polymer parameters (**Video 5**). Again, we observed chromatids segregation and disentanglement irrespective of fiber parameters and size of a single condensin molecule.

Our model makes several predictions that can be tested against available experimental data. First, in agreement with (36–39) the abundance of condensins on the chromosome significantly affects compaction and segregation of simulated chromatids (**Video 6**). While two-fold reduction of chromosome-bound condensins does not have a noticeable effect, upon ten and twenty-fold condensin depletion, chromosomes display poor compaction and diminished segregation.

Next, we examined the role of topological constraints and topo II enzyme in the process of chromosome compaction and segregation. Activity of topo II is modeled by a finite energy barrier for monomer overlap, allowing for occasional fiber crossings. We simulated topo II depletion by elevating the energy barrier and increasing the radius of repulsion between distant particles, thus reducing the rate of fiber crossings. In these simulations segregation of sister chromatids is drastically slowed down (**Video 7**). This effect of topological constraints on kinetics of compaction and segregation is expected since each chromosome is a chain with open ends that thus can eventually segregate from each other. We conclude that topo II is essential for rapid chromosome compaction, in accord with an earlier theoretical work (40) and with experimental observations (9, 41–43).

Finally, we examined the role of cohesin-dependent cohesion of chromosomal arms of sister chromatids. It is known that cohesins are actively removed from chromosomal arms in prophase. Interference with processes of cohesins removal or cleavage leads to compaction into elongated chromosomes that fail to segregate (44, 45). We simulated prophase compaction in the presence of cohesin rings (46) that stay on sister chromatids and can be pushed around by loop-extruding condensins. If cohesins remain uncleaved on sister chromatids (**Video 8**), we observe compaction of sister chromatids, that remain unsegregated, in agreement with experiment (44, 45).

Taken together, these results indicate that loop extrusion is sufficient to compact, disentangle and segregated chromosomes from a more open interphase state, to a compacted, elongated and linearly organized prophase state. Future Hi-C experiments focused on prophase chromosomes may be able to make detailed structural comparison with the prediction of our model.

Repulsion between loops shapes and segregates compacted chromatids.

Reorganization of chromosomes by loop extrusion can be rationalized by considering physical interactions between extruded loops. Excluded volume interactions and maximization of conformational entropy lead to repulsion of loops from each other (4, 47). They further stretch from the core and extend radially (**Figure 4**), similar to stretching of side chains in polymer “bottle-brushes” (48–50). This in turn leads to formation of the

bioRxiv preprint doi: https://doi.org/10.1101/038281; this version posted January 30, 2016. The copyright holder for this preprint (which was not certified by peer review) is the author/funder, who has granted bioRxiv a license to display the preprint in perpetuity. It is made available under aCC-BY-NC 4.0 International license.

central core where loop-bases accumulate (**Figure 4A**). Strong steric repulsion between the loops, caused by excluded volume interactions, stretches the core, thus maintaining linear ordering of loop bases along the genome (**Figure 2C**). Repulsion between loops also leads to stiffening of the formed loop-bottle-brush, as chromosome bending would increase overlaps between the loops.

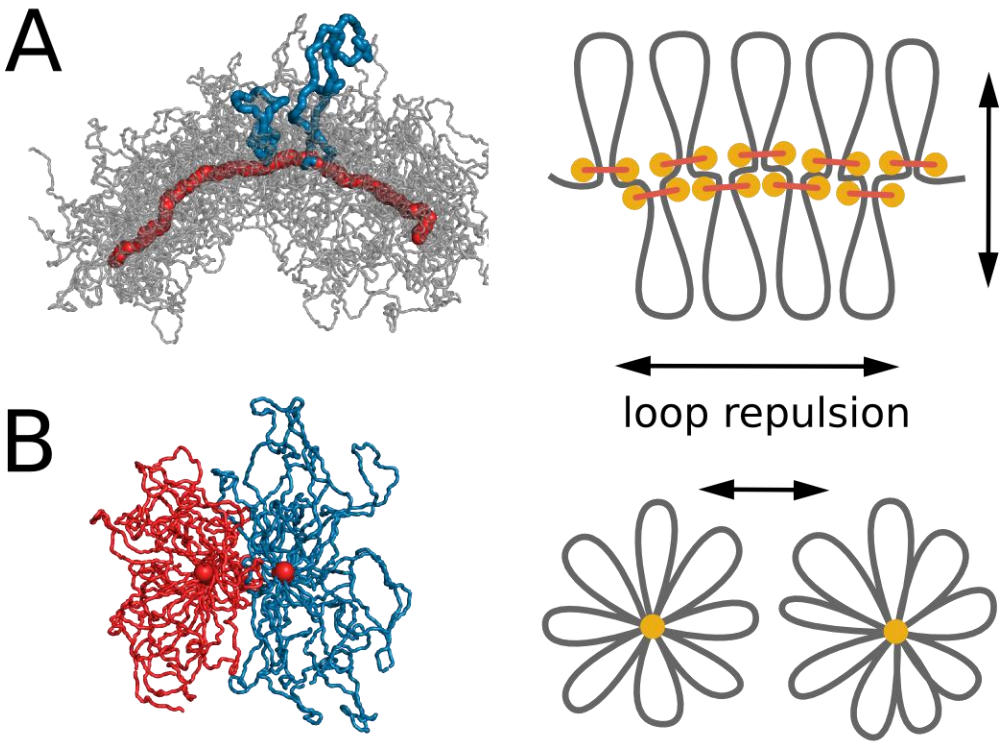

Figure 4. Steric repulsion between chromatin loops shapes the compacted chromosomes and leads to segregation of sister chromatids. (**A**) Left, conformation of a single chromosomes with chromatin fiber shown in semitransparent gray and condensins shown in red; two loops are highlighted with blue. Right: the diagram showing that loop repulsion straightens chromosomal cores and extends individual loops radially. (**B**) Left, cross section of two parallel loop brushes placed at a short distance from each other. Right, the diagram shows that steric interactions between loops of sister chromatids lead to chromatid repulsion and segregation.

Steric repulsion between loops of sister chromatid leads to segregation of sister chromatids that minimizes the overlap of their brush coronas (**Figure 4B**). Stiffening of the bottle-brush, in turn, leads to disentanglement of sister chromatids. To test this mechanism we performed simulations where excluded volume interactions have been turned off (**Video 5**). In these simulations, chromosomes did not assume a “bottle-brush” morphology and did not segregate, which confirms the fundamental role of steric repulsion for chromosome segregation.

Discussion

bioRxiv preprint doi: https://doi.org/10.1101/038281; this version posted January 30, 2016. The copyright holder for this preprint (which was not certified by peer review) is the author/funder, who has granted bioRxiv a license to display the preprint in perpetuity. It is made available under aCC-BY-NC 4.0 International license.

Our results show that chromosomal compaction by loop extrusion generates the major features of chromosome reorganization observed during prophase (2, 14). Loop extrusion leads to lengthwise *compaction* and formation of cylindrical, brush-like chromatids, reducing chromosome length by roughly 25-fold, while at the same time removing entanglements between separate chromatids. Unlike models of prophase *condensation* based on crosslinking of randomly colliding fibers (47, 51), chromatid compaction by loop extrusion exclusively forms bridges between loci of the same chromosome (**Figure 1A**). Similarly, loop-extrusion in bacteria, mediated by SMC proteins, was suggested to form intra-arm chromosomal bridges leading to lengthwise chromosome compaction (52, 53).

Our computations indicate that it takes an extended period of time for loop-extruding enzymes to maximally compact chromosomes. Maximal compaction is achieved by slow maturation of the loop array over multiple rounds of condensin exchange, rather than a single round of loop expansion. Loop length and the number of condensins per loop gradually increase during the maturation stage. Assuming that condensin II in prophase exchanges with the fast rate of condensin I in metaphase (~200 sec) (15) and using an average loop size of 100 kb, and an average spacing of condensins of 30 kb, it should take ~5 condensin exchange times, or about 17 minutes to achieve maximal compaction, which roughly agrees with the duration of prophase in human cells (54, 55). This gradual compaction also may explain why chromosomes of cells arrested in metaphase continue shrinking for many hours after the arrest (condensin II metaphase exchange time ~hours (15)).

Our model is idealized and does not aim to describe all of aspects of chromosome folding during mitosis. First, our model does not fully capture the specifics of later stages of mitosis. We model only the action of condensin II in prophase (56). Simple geometric considerations, Hi-C studies and mechanical perturbation of mitotic chromosomes show that, in metaphase, cells use additional mechanisms of lengthwise (axial) compaction.

Loop extrusion does not require specific interaction sites (e.g. loop anchors or condensin binding sites) and is therefore robust to mutations and chromosome rearrangements. This robustness also explains how a large segment of chromatin inserted into a chromosome of a different species can be reliably compacted by mitotic machinery of the host (57, 58). At the same time, this model allows the morphology of mitotic chromosomes to be tuned. Most importantly, the diameter and length of the simulated chromosomes depend on chromatin fiber properties as well as numbers of condensins [Supplemental Figure 3]; those dependences invite experimental tests.

In summary, we have shown that loop extrusion is a highly robust mechanism to compact, segregate and disentangle chromosomes. In a recent study (17) we also demonstrated that loop extrusion by another SMC complex, cohesin, could lead to formation of interphase topological association domains (TADs). We suggest that during interphase,

bioRxiv preprint doi: https://doi.org/10.1101/038281; this version posted January 30, 2016. The copyright holder for this preprint (which was not certified by peer review) is the author/funder, who has granted bioRxiv a license to display the preprint in perpetuity. It is made available under aCC-BY-NC 4.0 International license.

cohesins are sparsely bound, extruding 50-70% of DNA into highly dynamic loops, while metaphase condensins are bound more densely and more processive forming a dense array of stable loops. Taken together these studies suggest that loop extrusion can be a universal mechanism of genome folding, to mediate functional interactions during interphase and to compact during mitosis.

Acknowledgements

Work at NU was supported by the NSF through Grants DMR-1206868 and MCB-1022117, and by the NIH through Grants GM105847 and CA193419. Work at MIT was supported by the NIH through Grants GM114190, R01HG003143, and DK107980. We thank Elnaz Alipour, Job Dekker, Nancy Kleckner, the MIT Biophysics students and the members of Mirny Lab: Geoff Fudenberg, Nezar Abdennur, Christopher McFarland and, especially, E. M. Breville for stimulating and productive discussions.

References

1. Trask, B.J., S. Allen, H. Massa, and A. Fertitta. 1993. Studies of Metaphase and Interphase Chromosomes Using Fluorescence In Situ Hybridization. Cold Spring Harb Symp Quant Biol. 58: 767–775.
2. Nasmyth, K. 2001. Disseminating the genome: joining, resolving, and separating sister chromatids during mitosis and meiosis. Annu. Rev. Genet. 35: 673–745.
3. Marko, J.F. 2011. Scaling of Linking and Writhing Numbers for Spherically Confined and Topologically Equilibrated Flexible Polymers. J. Stat. Phys. 142: 1353–1370.
4. Marko, J.F., and E.D. Siggia. 1997. Polymer Models of Meiotic and Mitotic Chromosomes. Mol. Biol. Cell. 8: 2217–2231.
5. Marko, J.F. 2009. Linking topology of tethered polymer rings with applications to chromosome segregation and estimation of the knotting length. Phys. Rev. E. 79: 051905.
6. Marko, J.F. 2011. The Mitotic Chromosome : Structure and Mechanics. In: Rippe K, editor. Genome Organization and Function in the Cell Nucleus. Wiley-VCH Verlag GmbH & Co. KGaA. pp. 449–485.
7. Hirano, T., and T.J. Mitchison. 1993. Topoisomerase II does not play a scaffolding role in the organization of mitotic chromosomes assembled in Xenopus egg extracts. J. Cell Biol. 120: 601–12.
8. Hirano, T., and T.J. Mitchison. 1994. A heterodimeric coiled-coil protein required for mitotic chromosome condensation in vitro. Cell. 79: 449–458.
9. Wood, E.R., and W.C. Earnshaw. 1990. Mitotic chromatin condensation in vitro using somatic cell extracts and nuclei with variable levels of endogenous topoisomerase II. J. Cell Biol. 111: 2839–2850.
10. Hirano, T. 1995. Biochemical and genetic dissection of mitotic chromosome condensation. Trends Biochem. Sci. 20: 357–361.
11. Paulson, J.R., and U.K. Laemmli. 1977. The structure of histone-depleted metaphase chromosomes. Cell. 12: 817–828.
12. Earnshaw, W.C., and U.K. Laemmli. 1983. Architecture of metaphase chromosomes and chromosome scaffolds. J. Cell Biol. 96: 84–93.

bioRxiv preprint doi: https://doi.org/10.1101/038281; this version posted January 30, 2016. The copyright holder for this preprint (which was not certified by peer review) is the author/funder, who has granted bioRxiv a license to display the preprint in perpetuity. It is made available under aCC-BY-NC 4.0 International license.

13. Naumova, N., M. Imakaev, G. Fudenberg, Y. Zhan, B.R. Lajoie, L. a Mirny, and J. Dekker. 2013. Organization of the mitotic chromosome. Science. 342: 948–53.
14. Alipour, E., and J.F. Marko. 2012. Self-organization of domain structures by DNA-loop-extruding enzymes. Nucleic Acids Res. 40: 11202–12.
15. Gerlich, D., T. Hirota, B. Koch, J.-M. Peters, and J. Ellenberg. 2006. Condensin I stabilizes chromosomes mechanically through a dynamic interaction in live cells. Curr. Biol. 16: 333–44.
16. Goloborodko, A., J.F. Marko, and L. Mirny. 2015. Mitotic chromosome compaction via active loop extrusion. bioRxiv. .
17. Fudenberg, G., M. Imakaev, C. Lu, A. Goloborodko, N. Abdennur, and L.A. Mirny. 2015. Formation of Chromosomal Domains by Loop Extrusion. bioRxiv. .
18. Fukui, K., and S. Uchiyama. 2007. Chromosome protein framework from proteome analysis of isolated human metaphase chromosomes. Chem. Rec. 7: 230–7.
19. Jackson, D., P. Dickinson, and P.R. Cook. 1990. The size of chromatin loops in HeLa cells. EMBO J. 9: 567–71.
20. Yunis, J.J. 1981. Mid-prophase human chromosomes. The attainment of 2000 bands. Hum. Genet. 56: 293–298.
21. Sumner, A.T. 1991. Scanning electron microscopy of mammalian chromosomes from prophase to telophase. Chromosoma. 100: 410–418.
22. Yunis, J.J., and O. Sanchez. 1975. The G-banded prophase chromosomes of man. Hum. Genet. 27: 167–172.
23. Furey, T.S., and D. Haussler. 2003. Integration of the cytogenetic map with the draft human genome sequence. Hum. Mol. Genet. 12: 1037–1044.
24. Strukov, Y.G., and a S. Belmont. 2009. Mitotic chromosome structure: reproducibility of folding and symmetry between sister chromatids. Biophys. J. 96: 1617–28.
25. El-Alfy, M., and C.P. Leblond. 1989. An electron microscopic study of mitosis in mouse duodenal crypt cells confirms that the prophasic condensation of chromatin begins during the DNA-synthesizing (S) stage of the cycle. Am. J. Anat. 186: 69–84.
26. Sarkar, A., S. Eroglu, M.G. Poirier, P. Gupta, A. Nemani, and J.F. Marko. 2002. Dynamics of chromosome compaction during mitosis. Exp. Cell Res. 277: 48–56.
27. Kireeva, N., M. Lakonishok, I. Kireev, T. Hirano, and A.S. Belmont. 2004. Visualization of early chromosome condensation: a hierarchical folding, axial glue model of chromosome structure. J. Cell Biol. 166: 775–85.
28. Maeshima, K., M. Eltsov, and U.K. Laemmli. 2005. Chromosome structure: improved immunolabeling for electron microscopy. Chromosoma. 114: 365–75.
29. Maeshima, K., and U.K. Laemmli. 2003. A Two-Step Scaffolding Model for Mitotic Chromosome Assembly. Dev. Cell. 4: 467–480.
30. Marsden, M., and U. Laemmli. 1979. Metaphase chromosome structure: Evidence for a radial loop model. Cell. 17: 849–858.
31. Liang, Z., D. Zickler, M. Prentiss, F.S. Chang, G. Witz, K. Maeshima, and N. Kleckner. 2015. Chromosomes Progress to Metaphase in Multiple Discrete Steps via Global Compaction/Expansion Cycles. Cell. 161: 1124–1137.
32. Kleckner, N. 2006. Chiasma formation: chromatin/axis interplay and the role(s) of the synaptonemal complex. Chromosoma. 115: 175–194.
33. Poirier, M.G., and J.F. Marko. 2002. Mitotic chromosomes are chromatin networks without a mechanically contiguous protein scaffold. Proc. Natl. Acad. Sci. U. S. A. 99: 15393–7.
34. Oliveira, R.A., S. Heidmann, and C.E. Sunkel. 2007. Condensin I binds chromatin

bioRxiv preprint doi: https://doi.org/10.1101/038281; this version posted January 30, 2016. The copyright holder for this preprint (which was not certified by peer review) is the author/funder, who has granted bioRxiv a license to display the preprint in perpetuity. It is made available under aCC-BY-NC 4.0 International license.

early in prophase and displays a highly dynamic association with Drosophila mitotic chromosomes. Chromosoma. 116: 259–74.

35. Schwarzacher, H.G. 1976. Chromosomes: in Mitosis and Interphase. Berlin, Heidelberg: Springer Berlin Heidelberg. pp. 8–15.
36. Savvidou, E., N. Cobbe, S. Steffensen, S. Cotterill, and M.M.S. Heck. 2005. Drosophila CAP-D2 is required for condensin complex stability and resolution of sister chromatids. J. Cell Sci. 118: 2529–2543.
37. Steffensen, S., P.A. Coelho, N. Cobbe, S. Vass, M. Costa, B. Hassan, S.N. Prokopenko, H. Bellen, M.M.S. Heck, and C.E. Sunkel. 2001. A role for Drosophila SMC4 in the resolution of sister chromatids in mitosis. Curr. Biol. 11: 295–307.
38. Hagstrom, K.A., V.F. Holmes, N.R. Cozzarelli, and B.J. Meyer. 2002. C. elegans condensin promotes mitotic chromosome architecture, centromere organization, and sister chromatid segregation during mitosis and meiosis. Genes Dev. 16: 729–42.
39. Ono, T., D. Yamashita, and T. Hirano. 2013. Condensin II initiates sister chromatid resolution during S phase. J. Cell Biol. 200: 429–41.
40. Sikorav, J.L., and G. Jannink. 1994. Kinetics of chromosome condensation in the presence of topoisomerases: a phantom chain model. Biophys. J. 66: 827–837.
41. DiNardo, S., K. Voelkel, and R. Sternglanz. 1984. DNA topoisomerase II mutant of Saccharomyces cerevisiae: topoisomerase II is required for segregation of daughter molecules at the termination of DNA replication. Proc. Natl. Acad. Sci. . 81 : 2616–2620.
42. Newport, J., and T. Spann. 1987. Disassembly of the nucleus in mitotic extracts: Membrane vesicularization, lamin disassembly, and chromosome condensation are independent processes. Cell. 48: 219–230.
43. Shamu, C.E., and A.W. Murray. 1992. Sister chromatid separation in frog egg extracts requires DNA topoisomerase II activity during anaphase. J. Cell Biol. 117: 921–934.
44. Kueng, S., B. Hegemann, B.H. Peters, J.J. Lipp, A. Schleiffer, K. Mechtler, and J.-M. Peters. 2006. Wapl controls the dynamic association of cohesin with chromatin. Cell. 127: 955–67.
45. Gandhi, R., P.J. Gillespie, and T. Hirano. 2006. Human Wapl Is a Cohesin-Binding Protein that Promotes Sister-Chromatid Resolution in Mitotic Prophase. Curr. Biol. 16: 2406–2417.
46. Nasmyth, K., and C.H. Haering. 2009. Cohesin: Its Roles and Mechanisms. Annu. Rev. Genet. 43: 525–558.
47. Zhang, Y., and D.W. Heermann. 2011. Loops Determine the Mechanical Properties of Mitotic Chromosomes. PLoS One. 6: e29225.
48. Birshtein, T.M., O.V. Borisov, Y.B. Zhulina, A.R. Khokhlov, and T.A. Yurasova. 1987. Conformations of comb-like macromolecules. Polym. Sci. U.S.S.R. 29: 1293–1300.
49. Ball, R.C., J.F. Marko, S.T. Milner, and T.A. Witten. 1991. Polymers grafted to a convex surface. Macromolecules. 24: 693–703.
50. Li, H., and T.A. Witten. 1994. Polymers Grafted to Convex Surfaces: : 449–457.
51. Cheng, T.M.K., S. Heeger, R.A.G. Chaleil, N. Matthews, A. Stewart, J. Wright, C. Lim, P.A. Bates, and F. Uhlmann. 2015. A simple biophysical model emulates budding yeast chromosome condensation. Elife. 4.
52. Wang, X., T.B.K. Le, B.R. Lajoie, J. Dekker, M.T. Laub, and D.Z. Rudner. 2015. Condensin promotes the juxtaposition of DNA flanking its loading site in Bacillus subtilis. Genes Dev. . 29 : 1661–1675.

bioRxiv preprint doi: https://doi.org/10.1101/038281; this version posted January 30, 2016. The copyright holder for this preprint (which was not certified by peer review) is the author/funder, who has granted bioRxiv a license to display the preprint in perpetuity. It is made available under aCC-BY-NC 4.0 International license.

53. Wilhelm, L., F. Bürmann, A. Minnen, H.-C. Shin, C.P. Toseland, B.-H. Oh, and S. Gruber. 2015. SMC condensin entraps chromosomal DNA by an ATP hydrolysis dependent loading mechanism in Bacillus subtilis. Elife. 4.
54. Mora-Bermúdez, F., D. Gerlich, and J. Ellenberg. 2007. Maximal chromosome compaction occurs by axial shortening in anaphase and depends on Aurora kinase. Nat. Cell Biol. 9: 822–31.
55. Leblond, C.P., and M. El-Alfy. 1998. The eleven stages of the cell cycle, with emphasis on the changes in chromosomes and nucleoli during interphase and mitosis. Anat. Rec. 252: 426–443.
56. Hirota, T., D. Gerlich, B. Koch, J. Ellenberg, and J.-M. Peters. 2004. Distinct functions of condensin I and II in mitotic chromosome assembly. J. Cell Sci. 117: 6435–45.
57. Dietzel, S., and A.S. Belmont. 2001. Reproducible but dynamic positioning of DNA in chromosomes during mitosis. Nat Cell Biol. 3: 767–770.
58. Hirano, T., and T.J. Mitchison. 1991. Cell cycle control of higher-order chromatin assembly around naked DNA in vitro. J. Cell Biol. 115: 1479–1489.

bioRxiv preprint doi: https://doi.org/10.1101/038281; this version posted January 30, 2016. The copyright holder for this preprint (which was not certified by peer review) is the author/funder, who has granted bioRxiv a license to display the preprint in perpetuity. It is made available under aCC-BY-NC 4.0 International license.

Figure captions

Figure 1. Model of loop extrusion by condensins. Top row, the update rules used in simulations: (**A**) a condensin extrudes a loop by moving the two ends along the chromosome in the opposite directions, (**B**) collision of condensins bound to chromosomes blocks loop extrusion on the collided sides, (**C**) a condensin spontaneously dissociates and the loop disassembles; (**D**) a condensin associates at randomly chosen site and starts extruding a loop. Bottom row, (**E**) we study how combined action of many loop extruding condensins changes the conformation of a long chromosome using polymer simulations.

Figure 2. Loop-extruding condensins convert globular interphase chromosomes into elongated structures. (**A**) Dynamics of loop array formation. Left, the fraction of the chromosome extruded into loops (loop coverage, gray) and the mean loop size (black). The time is measured in the units of condensin residence time. Data for each curve was obtained using 10 simulation replicas; the thickness of each line shows the difference between the 10th and 90th percentile at each time point. Right, a phase diagram showing loop coverage vs mean loop length. The curve is averaged over the simulation replicas and colored by log-time. Two stages of dynamics are separated by the two vertical dashed lines corresponding to 95% coverage and 95% of the steady state mean loop length. The distinction between the two stages of compaction is especially easy to see on the phase curve. (**B**) Dynamics of chromosome morphology. Left: chromosome length (blue) and the mean chromosome diameter (red) shown as a function of time; the thickness of each line shows the difference between the 10th and 90th percentile at each time point. Right, a phase diagram showing chromosome length vs diameter; the curve is averaged over the simulation replicas and colored by log-time. Note that most of chromosome linear compaction is achieved during the first phase, while the second is characterized by widening of the chromosome and further three-fold shortening. (**C**) Snapshots of polymer simulations. Top row: the conformations of chromosomes at the beginning of simulations (left), slightly before the transition between the loop formation and maturation stages (middle), and in the steady state (right). Color (rainbow: from red to blue) shows positions of individual monomers along the chain and demonstrates that loci in compacted chromosomes are arranged linearly according to their genomic location. Bottom row: same as above, with chromosomes shown in semitransparent gray and condensins as red spheres.

Figure 3. Segregation and disentanglement of sister chromatids.
(**A**) The mean separation between sister chromosomes (blue) and the mean chromosome diameter (red) as a function of time, measured in condensin residence times, as above.
The blue band shows the range between 25th and 75th percentile at each time point; the light blue shows 10%--90% range. (**B**) Entanglement of sister chromatids measured by the linking number of the condensin cores of sister chromatids. (**C**) Conformations of two sister chromatids in the polymer simulations (shown in red and blue) illustrate the observed segregation and disentanglement.

Figure 4. **Steric repulsion between chromatin loops shapes the compacted chromosomes and leads to segregation of sister chromatids.** (**A**) Left, conformation of a single chromosomes with chromatin fiber shown in semitransparent gray and condensins shown in red; two loops are highlighted with blue. Right: the diagram showing that loop repulsion straightens chromosomal cores and extends individual loops radially. (**B**) Left, cross section of two parallel loop brushes placed at a short distance from each other. Right, the diagram shows that steric interactions between loops of sister chromatids lead to chromatid repulsion and segregation.

bioRxiv preprint doi: https://doi.org/10.1101/038281; this version posted January 30, 2016. The copyright holder for this preprint (which was not certified by peer review) is the author/funder, who has granted bioRxiv a license to display the preprint in perpetuity. It is made available under aCC-BY-NC 4.0 International license.

Video captions

Video 1: **An illustration of the model of loop extrusion by condensins**. When a condensin (red sphere) binds to chromatin (grey fiber), it binds to two adjacent loci and then slides the two contact points in the opposite directions, effectively extruding a loop (highlighted in orange). The diagram on the bottom shows the position of the two loci brought together by the condensin over time (red arc). Condensins occasionally unbind and then rebind to a randomly chosen site, starting a new loop. When two condensins (loops shown in orange and purple) meet on the chromosome, they stop extrusion on the collided sides. Condensins can also bind within already extruded loops. If the growth of the outer loop is blocked by other loops or barriers (not shown), the inner condensin can re-extrude it, forming a single loop reinforced by multiple condensins (the number above the arc). Such a loop is stabilized against unbinding of individual condensins and disassembles only upon unbinding of the last condensin. Available at https://www.youtube.com/watch?v=xikxZ0yF1yU&list=PLnV-JMzdy0ZMOvyK6Z1bzU7C2Jt8Brbit&index=1

Video 2: A representative polymer simulation of compaction of 30 Mb chromosome by loop extruding condensins in presence of strand-passing topo II. Top left, fiber color corresponds to the position of each monomer along the genome. Top right, fiber shown in semitransparent gray, condensins are shown as red spheres. Bottom, the diagram of the crosslinks (red arcs) formed by condensins. The numbers above the arcs show the number of condensins stacked at the bases of reinforced loops. We sped up the second half of the video 20 times to illustrate the slow phase of loop maturation and the long-term stability of the compacted state. Available at https://www.youtube.com/watch?v=_Vc7__xfnfc&list=PLnV-JMzdy0ZMOvyK6Z1bzU7C2Jt8Brbit&index=2

Video 3: A polymer simulation of segregation and disentanglement of two sister chromatids by loop extruding condensins in presence of strand-passing topo II. The two sister chromatids (30Mb each) are shown in red and blue. Initially, the two chromatids were compacted and twisted around each other. Second half of the video is sped up 20x. Available at https://www.youtube.com/watch?v=stZR5s9n32s&index=3&list=PLnV-JMzdy0ZMOvyK6Z1bzU7C2Jt8Brbit

Video 4: Sixteen simulation replicas of chromatid segregation and disentanglement. Available at https://www.youtube.com/watch?v=UXXLnGGit-8&index=4&list=PLnV-JMzdy0ZMOvyK6Z1bzU7C2Jt8Brbit

Video 5: Polymer simulation of segregation and disentanglement of two sister chromatids with altered model parameters. Top row: left, simulations with a more flexible fiber (0.5x bending energy); right – a stiffer fiber (2x bending energy); bottom row, left - simulations with wider condensins at loop bases; right – simulations with disabled excluded volume interactions. Available at https://www.youtube.com/watch?v=YhgSHppJXVI&index=5&list=PLnV-JMzdy0ZMOvyK6Z1bzU7C2Jt8Brbit

Video 6: Polymer simulation of segregation and disentanglement of two sister chromatids with reduced condensin abundance. Top row, left - 500 condensins per chromatid; right - 200 condensins; bottom row, left - 100 condensins; right, 50 condensins. Available at https://www.youtube.com/watch?v=oq9TS5OXO1Q&index=6&list=PLnV-JMzdy0ZMOvyK6Z1bzU7C2Jt8Brbit

bioRxiv preprint doi: https://doi.org/10.1101/038281; this version posted January 30, 2016. The copyright holder for this preprint (which was not certified by peer review) is the author/funder, who has granted bioRxiv a license to display the preprint in perpetuity. It is made available under aCC-BY-NC 4.0 International license.

Video 7: A polymer simulation of segregation and disentanglement of two sister chromatids upon topo II depletion. Depletion of topo II was simulated by a simultaneous increase of the energy barrier of fiber overlap and the increased radius of repulsion, which decreased, but not fully prevented chain crossings. Available at https://www.youtube.com/watch?v=YO3Qx8liK3s&list=PLnV-JMzdy0ZMOvyK6Z1bzU7C2Jt8Brbit&index=7

Video 8: **A polymer simulation of segregation and disentanglement of sister chromatids in the presence of cohesins connecting the chromatids.** We simulated cohesins as crosslinks between the chromosomes (shown with the blue lines on the bottom arc diagram) that can be pushed along each of the chromatids by loop-extruding condensins. Available at https://www.youtube.com/watch?v=vmwNbz41pqM&list=PLnV-JMzdy0ZMOvyK6Z1bzU7C2Jt8Brbit&index=8